Real-Time Energy Management Strategy of a Fuel Cell Electric Vehicle With Global Optimal Learning

Shengyan Hou, Hai Yin, Benjamín Pla, Jinwu Gao, and Hong Chen, *Fellow, IEEE*

***Abstract*— This article proposes a novel energy management strategy (EMS) for a fuel cell electric vehicle (FCEV). The strategy combines the offline optimization and online algorithms to guarantee optimal control, real-time performance, and better robustness in an unknown route. In particular, dynamic programming (DP) is applied in a database with multiple driving cycles to extract the theoretically optimal power split between the battery and fuel cell with a priori knowledge of the driving conditions. The analysis of the obtained results is then used to extract the rules to embed them in a real-time capable fuzzy controller. In this sense, at the expense of certain calibration effort in the offline phase with the DP results, the proposed strategy allows on-board applicability with suboptimal results. The proposed strategy has been tested in several actual driving cycles, and the results show energy savings between 8.48% and 10.71% in comparison to rule-based strategy and energy penalties between 1.04% and 3.37% when compared with the theoretical optimum obtained by DP. In addition, a sensitivity analysis shows that the proposed strategy can be adapted to different vehicle configurations. As the battery capacity increases, the performance can be further improved by 0.15% and 1.66% in conservative and aggressive driving styles, respectively.**

***Index Terms*— Battery capacity sensitivity, dynamic programming (DP), energy management, fuel cell electric vehicles (FCEVs), fuzzy rule learning (FRL).**

NOMENCLATURE

E_b	Battery energy.
$E_{H_2,l}$	Lower heating value of hydroge.
P_b	Battery power.
$P_{b,\max}$	Battery maximum power.
$P_{b,\min}$	Battery minimum power.
P_{de}	Vehicle power demand.
P_{fc}	Fuel cell power.
$P_{\text{fc,max}}$	Fuel cell maximum power.
R_b	Battery resistance.
SOC	Battery state of charge.
$\text{SOC}_{\min}$	Maximum state of charge.
$\text{SOC}_{\max}$	Minimum state of charge.
SOC_{t_0}	Initial state of charge.
SOC_{t_f}	End state of charge.
T	Duration of driving cycle.
Q_m	Battery capacity.
ΔSOC	Battery SOC variation.
$U_{b,\text{oc}}$	Battery OCV voltage.
I_b	Battery current.
m	Mass of the FCEV.
$\dot{m}_{\text{fc}}$	Hydrogen consumption.
η_{fc}	FCS efficiency.
$\overline{\eta}_{\text{fc}}$	FCS average efficiency.
c	Mean value of the GMF.
σ	Variance of the GMF.

Shengyan Hou and Jinwu Gao are with the State Key Laboratory of Automotive Simulation and Control and the Department of Control Science and Engineering, Jilin University, Changchun 130025, China (e-mail: gaojw@jlu.edu.cn).

Hai Yin is with the State Key Laboratory of Automotive Simulation and Control, Jilin University, Changchun 130025, China.

Benjamín Pla is with the CMT-Motores Térmicos, Universitat Politècnica de València, 46022 Valencia, Spain.

Hong Chen is with the Department of Control Science and Engineering, Jilin University, Changchun 130025, China, and also with the Department of Control Science and Engineering, Tongji University, Shanghai 200092, China.

I. INTRODUCTION

FUEL cell electric vehicles (FCEVs), utilizing hydrogen instead of diesel and gasoline as power fuels, are a kind of clean energy vehicles with the advantages of high-energy conversion efficiency, low noise, and zero exhaust emissions [1], [2], [3]. Because FCEVs are necessary equipped with an auxiliary energy source to realize the power demand for transient peak and recovery of braking energy, the energy management strategy (EMS) is indispensable [4], [5]. However, highly nonlinear system on different timescales, uncertainty in driving conditions and heavy computational load pose major obstacles in EMS design [6], [7], [8]. Consequently, an appropriate and effective EMS implementing optimal control, real-time performance, and better robustness in FCEVs play an essential role in improving the powertrain efficiency.

Due to the current interest about the topic, an extensive literature can be found and the reported EMSs can be classified into three categories: 1) rule-based [9], [10]; 2) optimization-based [11], [12]; and 3) reinforcement learning (RL)-based [13], [14]. The rule-based EMSs, designing by professional knowledge or engineering experience, dynamically adjust the power distribution between the energy sources according to the driving conditions, to ensure that the fuel cell operates at its optimal efficiency [15]. In [16], a real-time strategy based on multimode was proposed for a FCEV to improve the efficiencies of each energy source and reduce

the degradation rate of the fuel cell. A heuristic control strategy based on rule logic was presented in [17]. Through appropriate normalization and denormalization techniques, the control rules could be applied to a variety of FCEV powertrain systems. As an extension of deterministic rules, fuzzy logic combines expert experience to rules and does not depend on the precise mathematical model of the controlled object. In [51], a fuzzy rule control strategy regulated the FC and battery output power under different driving conditions. To maximize the system efficiency and to minimize the battery current variation, an adaptive fuzzy logic-based EMS was designed in [19]. Although their designs are simple and easy to implement, these strategies usually need to design EMSs based on experience. The results are not optimal, and there is a problem of insufficient adaptability to driving cycles [20].

In addition, the optimization-based EMSs are usually used to more effectively reduce hydrogen consumption, increase the fuel cell life span, and increase the driving mileage [21], [22]. According to the different dependence on prior knowledge, the optimization-based EMSs can be divided into global and instantaneous optimization methods. Specifically, the global optimization algorithm mainly includes dynamic programming (DP), Pontryagin's minimum principle (PMP), and genetic algorithm. A bi-loop DP algorithm was proposed in [23], which could simultaneously optimize the EMS and battery capacity, as well as analyze the impact of the discrete step size of DP on the accuracy and computing load. A real-time and suboptimal EMS based on PMP for FCEVs was studied in [24], and an online adjoint state update method was also proposed. In [25], an intelligent EMS combining genetic algorithm and quadratic programming was presented to improve the fuel economy of a hybrid electric vehicle. To solve the finite-time horizon EMS optimal control problem of hybrid electric vehicles, Wu et al. [26] developed a logical network-based algorithm that is designed based on the semi-tensor product of the matrix, and a series of simulation results validated its effectiveness. However, due to the large computational load and heavy dependence on driving conditions, the global optimization algorithm is difficult to apply in practice. Usually, its results serve as a benchmark for evaluating policies and formulating rules. The instantaneous optimization methods mainly include the equivalent consumption minimization strategy (ECMS), model predictive control (MPC), and so on. Geng et al. [27] studied the EMS of fuel cell and battery hybrid vehicles based on the ECMS to achieve better hydrogen economy. Nonetheless, the key challenge is to estimate the equivalent factor (EF) based on components' characteristics and dynamics of energy sources, since the EF plays a substantial role in ECMS performance. Focus on this problem, Peng et al. [1] derived a quantitative analytical formula to determine the EF based on the SOC and the average fuel cell power using the optimal control theory. The performance was demonstrated by comparison to the offline PMP-based strategies. By transforming the global optimal problem into a local optimization problem in the prediction horizon, the MPC-based EMS continuously updates the future state through rolling optimization to obtain the optimization results. In [28], an EMS based on nonlinear MPC was designed for FCEVs and employed a recurrent neural network for modeling a proton exchange membrane fuel cell (PEMFC). The results indicated that the MPC improved hydrogen economy and reduced fuel cell degradation. However, developing accurate mathematical models for achieving preferable solutions is an imperative premise of these instantaneous optimization algorithms.

As a potential solution to real-time optimization challenges, RL methods have attracted significant attention. RL agents take action based on the accumulation of long-term rewards. Therefore, a well-trained RL agent is capable of predicting system evolution and guarantee optimal control. It has been demonstrated that RL is an efficient method to manage the energy of hybrid electric vehicles [29], [30]. In [31], a thorough parametric study was conducted on four key factors during the Q-learning-based EMS development. To solve the discrete state variables problem, Wu et al. [32] proposed a deep Q network (DQN)-based EMS for a hybrid electric bus, and their results showed that DQN performed better than the traditional Q-learning model. Lian et al. [33] proposed an improved optimization framework for EMSs that integrated expert knowledge into the deep deterministic policy gradient algorithm and solved the problem of a large space of control variables. Sun et al. [34] proposed a hierarchical energy splitting structure to shrink the state-action space based on an adaptive fuzzy filter, and the reinforcement-learning combining ECMS was presented for tackling the high-dimensional state-action space. However, sparse rewards are common seen when using RL. Qi et al. [35] studied a novel RL-based method for EMSs. Through this new algorithm, they not only solved the problem of sparse reward in the training process, but also achieved the optimal power distribution. However, the RL-based EMS needs to learn from feedback reward and penalty signals, and it often has characteristics such as noise and delay.

Accordingly, the current EMS suffers from the inferiorities of a high-computational cost burden, unsatisfactory optimization performance, and poor robustness [36], [37]. A highly effective EMS should guarantee the optimal control, real-time performance, and better robustness while is applicable in practice. Global optimization algorithms, such as DP, can obtain the optimal energy consumption results under certain driving conditions, but they are difficult to apply in real time. The rule-based EMSs are easy to guarantee fast implementation, but the design of rules mainly relies on expert experience or prior knowledge and has poor adaptability. A breakthrough could be to explore effective EMSs that can enhance algorithm's strengths and compensate for their deficiencies. Moreover, rule learning algorithm, as a branch of machine learning, has the advantages of less reliance on expert experience, unnecessary requirements for prior knowledge, strong capability of learning, and portability, which has been widely applied in industry. Therefore, it would be a problem worth solving to combine DP and fuzzy rules using rule learning to design an easy-to-implement online EMS. It can

overcome the limitations of the requirement for engineering experience in traditional rule-based EMSs and prior driving information in optimization-based EMSs. To the authors' knowledge, there are only a few papers on fuzzy rule learning (FRL) based on theoretical optimization. An improved rule-based EMS depending on DP and maintaining SOC was developed in [38], but the rules were determined artificially according to DP global solutions. Liu et al. [39] and [40] proposed an EMS based on rule learning according to PMP optimization results, and the parameters for fitting rules were solved by the Broyden–Fletcher–Goldfarb–Shanno algorithm. Nevertheless, the accuracy of the PMP algorithm depends on the co-states factor, and the sensitivity of the designed strategy to changes in the component parameters is not analyzed. Jia et al. [41] proposed a series fuzzy control strategy to decrease the current fluctuation and improve the durability of the fuel cell system (FCS). Meanwhile, to increase the driving mileage, the optimal membership function and fuzzy rule weight were found based on particle swarm optimization. However, the designed strategy cannot obtain approximate optimal results.

Therefore, aiming at eliminating the uncertainty of expert experience in the fuzzy controller, and combining the advantages of the fuzzy rule control strategy and DP algorithm, this article presents an EMS based on FRL. First, four standard driving cycles are selected to establish the optimal database based on the DP algorithm as the optimal sample database for FRL. The input and output data of the fuzzy controller are divided into five classes by the hierarchical clustering method, and the membership function is designed according to the classification results of optimal database. The repeated incremental pruning is performed based on the decision tree algorithm to eliminate redundant data and avoid overfitting of rule learning. Then the multiple linear regression model is applied to identify the parameters of learned rules. Finally, the influence of battery capacity change on the proposed strategy is analyzed, and the adaptability of FRL to different battery capacities is also given.

In brief, there are three contributions in this study.

1) Rules and membership functions of fuzzy rule controller are learned from optimal data, and none of them require expert knowledge.
2) The proposed algorithm is designed under the framework of optimization theory to guarantee the suboptimal control, and its results are only 1.12%–4.13% higher than the global optimum.
3) The proposed strategy has good robustness and can maintain a good energy-saving effect when the battery parameters are changed.

The structure of the remainder of this article is as follows. The EMS optimal control problem is presented in Section II, including the model description and the problem formulation. Section III describes the EMS based on FRL, which aims to achieve approximate optimality of the proposed strategy. In Section IV, it analyses the simulation results and evaluates the effectiveness of the EMS based on FRL. Finally, the main conclusion are drawn in Section V.

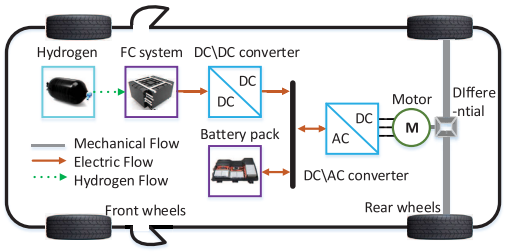

Fig. 1. FCEV configuration.

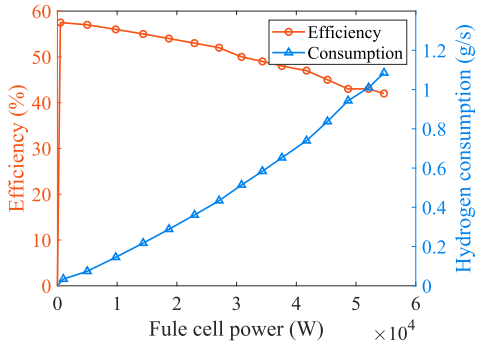

Fig. 2. FCS efficiency and hydrogen consumption.

II. Model Description and Problem Formulation

The powertrain structure of the FCEV studied in this article is shown in Fig. 1, and the parameters of the FCEV are listed in Table I, which are provided by the Dongfeng Motor Corporation. It is mainly composed of a FCS, a battery, a motor, a unidirectional dc–dc converter, and a dc–ac traction inverter. The FCS is connected to the dc bus through the dc–dc converter to provide the main energy for the vehicle. The battery, as an auxiliary energy source, improves the dynamic response of the powertrain system.

A. Fuel Cell System

A fuel cell is a clean and efficient power generation device that converts the chemical energy in hydrogen into electrical energy. The type of fuel cell in this study is a PEMFC. The fuel cell model for energy optimization is a static model which neglects dynamic behavior. It is enough to analyze vehicle energy and estimate fuel consumption using this model [42], [43]. The model mainly includes efficiency models and hydrogen consumption models, as shown in Fig. 2.

The hydrogen consumption of the FCS is determined by the power and corresponding efficiency, which can be seen in the equation as follows:

$$\dot{m}_{\mathrm{fc}} = \frac{1}{E_{H_2,l}} \int \frac{P_{\mathrm{fc}}}{\eta_{\mathrm{fc}}(P_{\mathrm{fc}})}\, dt. \tag{1}$$

In the current article, the integral (1) is replaced by a discrete approximation with a time-step of 1 s.

B. Battery System

Batteries have gradually become one of the important components in today's electric vehicles. They can not only "cut

TABLE I

PARAMETERS OF THE FCEV

Parameter	Symbol	Value
Vehicle mass	m	1815.9 kg
Wheel radius	r_w	334 mm
Rolling coefficient	c_r	0.0074
Drag coefficient	C_D	0.371
Vehicle frontal area	A	2.65 m^2
Final gear ratio	i_0	9.061
FC, Cell count	–	300
FC, Rated power	$P_{fc,rat}$	41.4 kW
FC, Rated voltage	$U_{fc,nom}$	180 V
FC, Maximum voltage	$U_{fc,max}$	339 V
FC, Maximum power	$P_{fc,max}$	60 kW
FC, Rated current	$I_{fc,rat}$	230 A
B, Series and Parallel	–	96S3P
B, Cell capacity	Q_m	21600 As
B, Nominal voltage	U_{nom}	350 V
B, Maximum power	$P_{b,max}$	70 kW
B, Minimum power	$P_{b,min}$	-70 kW

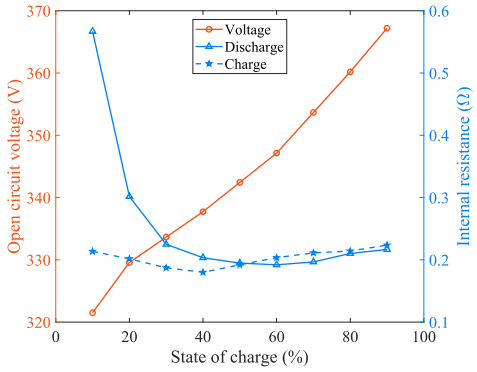

(a)

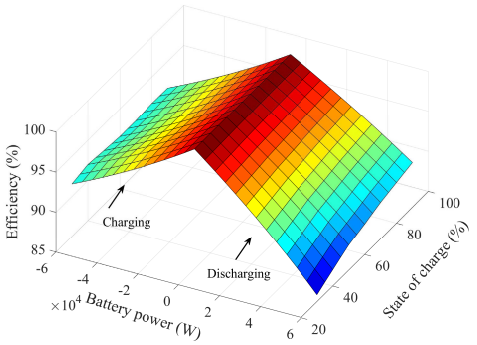

(b)

Fig. 3. Numerical model characteristics of the battery system. (a) Open circuit voltage and internal resistance. (b) Charging and discharging efficiency.

peaks and fill valleys" for the required power when outputting, but also recover braking energy when the vehicle is braking downhill, which improves the economy of the vehicle [44].

Following the main trend in the EMS, the battery is represented by an R-int model, which is simple but effective, composed of a variable resistor and a voltage source in series [45], as shown in Fig. 3. The battery output power P_b from the equivalent circuit is

$$P_b = U_{b,\mathrm{oc}} I_b - R_b I_b^2. \tag{2}$$

According to the model (2), the battery current I_b is a function of the open circuit voltage, output power, and internal resistance of the battery as follows:

$$I_b = \frac{U_{b,\mathrm{oc}} - \sqrt{U_{b,\mathrm{oc}}^2 - 4R_b P_b}}{2R_b}. \tag{3}$$

The battery SOC is calculated by the ampere-hour integral method, and the SOC transfer equation is as follows:

$$\dot{\mathrm{SOC}} = -\frac{I_b}{Q_m}. \tag{4}$$

C. Mathematical Description of the Optimization Problem

For designing the EMS of FCEVs, the goal is to optimize the split between battery and fuel cell power to minimize the fuel consumption in the entire time domain. We suppose the control variable u is P_{fc} and the state variable x is SOC; then, the optimization problem can be described as follows:

$$J = \int_1^T \dot{m}_{\mathrm{fc}}(t)dt. \tag{5}$$

Combining the energy balance in the FCEV (see Fig. 1) with equations (3) and (4), the SOC dynamics can be represented as follows:

$$\dot{\mathrm{SOC}} = -\frac{U_{b,\mathrm{oc}} - \sqrt{U_{b,\mathrm{oc}}^2 - 4R_b(P_{\mathrm{de}} - P_{\mathrm{fc}})}}{2Q_m R_b}. \tag{6}$$

The elements in the FCEV powertrain are subject to their own limitations in terms of performance, and the vehicle must maintain the battery SOC to avoid eliminating the potential for energy savings in the future. In the different driving conditions, start-stop, high load, low load, and variable load operations degrade the internal physical and chemical materials of fuel cells, which negatively affects performance. The dynamic response constraints of fuel cells, $\Delta P_{\mathrm{fc,max}} = 3$ kW/s, should be considered in energy optimization problem. Thus, the powertrain system constraints are as follows:

$$\begin{cases} 0 \le P_{\mathrm{fc}} \le P_{\mathrm{fc,max}} \\ -\Delta P_{\mathrm{fc,max}} \le \Delta P_{\mathrm{fc}} \le \Delta P_{\mathrm{fc,max}} \\ P_{b,\mathrm{min}} \le P_b \le P_{b,\mathrm{max}} \\ \mathrm{SOC}_{\mathrm{min}} \le \mathrm{SOC} \le \mathrm{SOC}_{\mathrm{max}}. \end{cases} \tag{7}$$

III. FRL EMS BASED ON PARAMETERS LEARNING AND RULES EXTRACTION

As mentioned in the introduction, fuzzy control is a control method with easy implementation and convenience, but the design of rules relies on expert experience and cannot guarantee optimality. DP can guarantee the global optimality, but it must use all the driving cycles information. It also has the disadvantage of the curse of dimensionality [46], [47]. Considering the complementarity between fuzzy control and DP, this study designs an FRL algorithm for EMS of FCEVs. The FRL mainly includes establishing the optimal database,

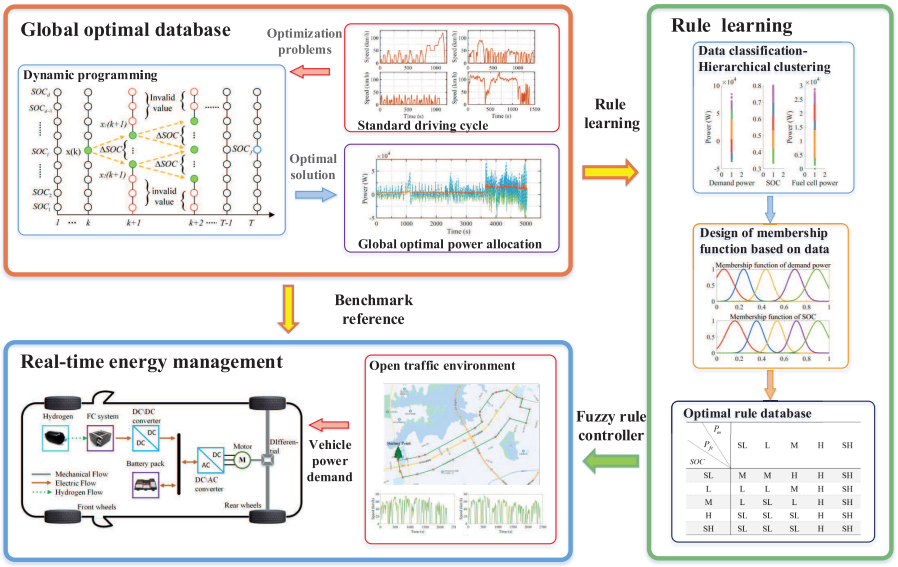

Fig. 4. Block diagram of FRL.

learning fuzzy controller parameters, and designing the rule based on data. The block diagram of FRL is depicted in Fig. 4. Moreover, the optimal database is based on the optimal results of DP, and the goal is to learn on the basis of the optimal benchmark. Automatically learning of the fuzzy rules from the data extracted from the optimal solutions obtained by DP, avoids the subjectivity brought by expert experience to the greatest extent. The global optimum is obtained by the DP algorithm that needs to preview all distance information. Theoretically, any optimization- or rule-based strategy in the short horizon cannot obtain the global optimum, but other methods differ in the ability to guarantee the global optimality. In this article, a FRL algorithm is proposed to solve the energy optimization problem for FCEVs, which simplifies the algorithm design process and guarantee the sub-optimality. Moreover, there are different outputs for the same input in the optimal database, because the global driving cycles need to be previewed to obtain this result. When there is only short horizon information of driving cycles, the membership function designed by the clustering method and the fuzzy rules extracted from the database can guarantee the sub-optimality to the greatest extent. Therefore, the methodology in this article aims at guaranteeing the sub-optimality.

A. Global Optimal Database Establishment

The optimization-based EMS requires high model accuracy, especially the optimization method for online applications. When the database is established offline, a more complex model can be used to ensure that the method can guarantee global optimal control, which should be more flexible than using online. The new european driving cycle (NEDC), urban dynamometer driving schedule (UDDS), manhattan (MAN), and representative non-LA4 cycle (REP05) driving cycles are combined into one, and the optimal database is derived from the energy optimization results of the DP algorithm under the combined driving cycle. Equations (5)–(7) are discretized with a time-step of 1 s, and the optimization problem based on DP algorithm is defined as follows:

$$
\begin{aligned}
&\min_{P_{\mathrm{fc}}(\cdot)} \sum_{k=1}^{T} \dot{m}_{\mathrm{fc}}(k)\Delta t \\
&\text{s.t.: } \mathrm{SOC}(k+1) = \mathrm{SOC}(k) \\
&\qquad - \frac{U_{b,\mathrm{oc}}(k) - \sqrt{U_{b,\mathrm{oc}}(k)^2 - 4R_b(k)P_b(k)}}{2Q_m R_b(k)}\Delta t \\
&\qquad P_{\mathrm{fc}}(k) + P_b(k) = P_{\mathrm{de}}(k) + P_a \\
&\qquad 0 \le P_{\mathrm{fc}}(k) \le P_{\mathrm{fc,max}} \\
&\qquad \Delta P_{\mathrm{fc,min}} \le \Delta P_{\mathrm{fc}}(k) \le \Delta P_{\mathrm{fc,max}} \\
&\qquad P_{b,\mathrm{min}} \le P_b(k) \le P_{b,\mathrm{max}} \\
&\qquad \mathrm{SOC}_{\mathrm{min}} \le \mathrm{SOC}(k) \le \mathrm{SOC}_{\mathrm{max}} \\
&\qquad \mathrm{SOC}(1) = \mathrm{SOC}(T)
\end{aligned} \tag{8}
$$

where P_{de} denotes the power demand of the vehicle, and $P_a = 1$ kW is the auxiliary power. Fig. 5 shows the velocity trajectories of four driving cycles and the optimization results based on the DP.

However, in different time periods of driving cycles, when the demand power and the battery SOC at the later time are the same as the previous, the results obtained by DP sometimes are very different just because the future demand power is different. This difference is caused by the noncausality of the DP algorithm. This problem in practical applications is eliminated by analyzing the database and calculating the probability, which is discussed in Section III-C. The optimal results of the combined driving cycle are used as the optimal database for the next step of fuzzy controller parameter setting and rule learning.

B. Fuzzy Controller Parameter Learning

The Takagi-Sugeno (T-S) fuzzy controller is selected in this article, the input is the demand power of the FCEV and the SOC of the battery, and the fuel cell power is the controller

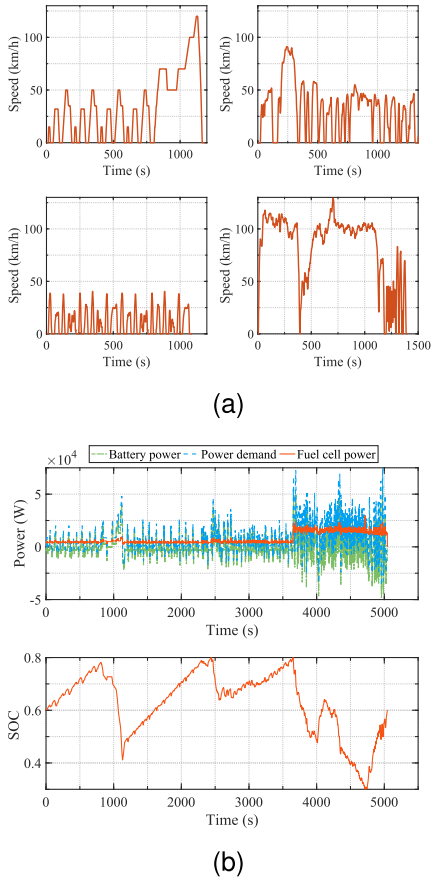

Fig. 5. Velocity trajectories and energy distributions of driving cycles in the optimal database. (a) Velocity trajectories of four driving cycles. (b) EMS results based on the DP algorithm.

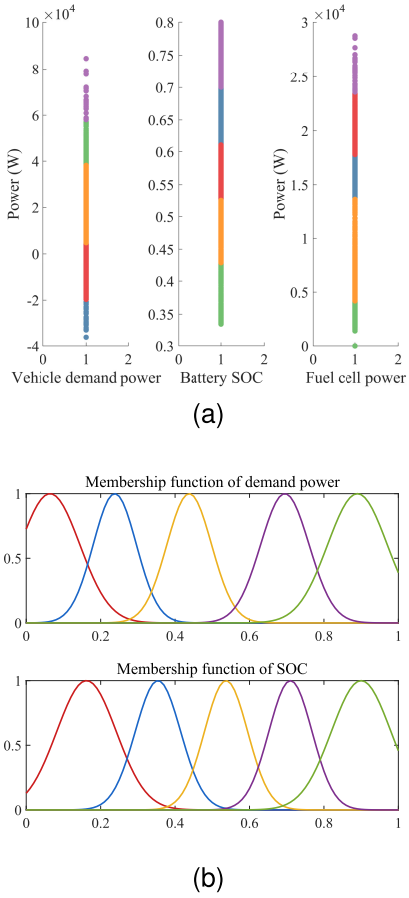

Fig. 6. Classification and membership degree of optimal data. (a) Clustering results of the optimal database. (b) Membership function according to the clustering results.

output. In fuzzy control, it is necessary to convert the input precise value into fuzzy language variables for the next step of fuzzy rule judgment, which requires the membership function to convert the input precise value, which is fuzzification. The Gaussian membership function (GMF) is selected in the design of the fuzzy controller, whose smoothness and accuracy are between the triangular and trapezoidal membership functions. The general GMF expression is as follows:

$$\mu(\gamma) = e^{-\frac{(\gamma-c)^2}{2\sigma^2}}. \tag{9}$$

To effectively distinguish the types of input data, the data need to be processed by the hierarchical clustering method. The results of the DP are used to classify the driving cycles and vehicle state in terms of the input variable (power demand and SOC). The hierarchical clustering method is based on distance to classify and to determine the similarity between each data point in the database, and the distance calculation uses the Euclidean distance calculation method as follows:

$$\mathrm{dist}(\alpha, \beta) = \sqrt{\sum_{i=1}^{N} (\alpha_i - \beta_i)^2} \tag{10}$$

where $\mathrm{dist}(\alpha, \beta)$ is the Euclidean distance of α and β, and the clustering method adopts the weighted average method.

The input and output data of the fuzzy controller are divided into five categories by the hierarchical clustering method. Although the number of classifications is determined, the c and σ of the membership function are determined according to the data clustering results. The classification result is shown in Fig. 6(a). This article uses the method of hierarchical clustering instead of expert experience as the design membership function, which is an effective way to design the membership function. Since hierarchical clustering divides the data set into five categories, the number of GMFs input by this fuzzy controller is also set to 5. The input is normalized. The parameters c and σ of the GMF are set as the mean and variance of each clustering result of the database. The input membership functions after optimizing are as shown in Fig. 6(b).

C. Rules Design Based on the Data

After the membership function is determined, next is the rule design. The impact of the DP noncausality mentioned in Section III-A brings challenges to the rules design, which will be solved by the repeated incremental pruning based on the decision tree algorithm. The rules design based on decision tree involves an iterative process of data pair (attribute-value) selection.

In the rules design, the data set of fuel cell power involves five categories, which are very low (“SL”), low (“L”), medium (“M”), high (“H”), and very high (“SH”), and thus, a set

TABLE II

FREQUENCY OF THE FUEL CELL POWER AND THE VEHICLE POWER DEMAND

P_{fc}	$P_m = SL$	$P_m = L$	$P_m = M$	$P_m = H$	$P_m = SH$
SL	0	1518	318	0	0
L	23	883	922	23	0
M	6	298	214	0	0
H	0	0	656	134	1
SH	0	0	0	7	43
Total	29	2699	2110	164	44

TABLE III

CONDITIONAL PROBABILITY OF THE FUEL CELL OUTPUT AND THE VEHICLE POWER DEMAND

P_{fc}	$P_m = SL$	$P_m = L$	$P_m = M$	$P_m = H$	$P_m = SH$
SL	0	1518/2699	318/2110	0	0
L	23/29	883/2699	922/2110	23/164	0
M	6/29	298/2699	214/2110	0	0
H	0	0	656/2110	134/164	1/44
SH	0	0	0	7/164	43/44

TABLE IV

CONDITIONAL PROBABILITY OF BATTERY SOC WHEN $P_{\text{fc}} = \text{SL}$ AND $P_m = L$

Battery SOC	$P_{fc} = SL$ and $P_m = L$
SL	0
L	3/1518
M	84/1518
H	598/1518
SH	833/1518

TABLE V

FUZZY CONTROL RULES AFTER LEARNING

P_{fc} \ P_M / SOC	SL	L	M	H	SH
SL	M	M	H	H	SH
L	L	L	M	H	SH
M	L	SL	L	H	SH
H	SL	SL	SL	H	SH
SH	SL	SL	SL	H	SH

of rules for the five output categories should be designed. The design process should lead to only one relation between the fuzzy controller inputs and outputs. Through the statistics of the database, the frequency table of the output and the input attributes can be obtained, as shown in Table II. Then, the conditional probability that the fuel cell power belongs to different classes of the power demand can be calculated according to the frequency table, as shown in Table III.

When the output power P_{fc} of the fuel cell is "SL," that is, the output is very small, and the maximum value of the conditional probability is selected at this time. Among the five groups of conditional probabilities, the conditional probability is the largest when $P_m = L$, and $P(P_{\text{fc}} = \text{SL} \mid P_m = L) = 1518/2699$. However, when $P_m = L$, $P_{\text{fc}} = \text{SL}$ is not completely established, the rule still needs to be learned down to make further rule distinctions. 1518 examples are extracted that satisfy $P_{\text{fc}} = \text{SL} \mid P_m = L$ from the database, and the conditional probability of the next level of input SOC can be obtained, as shown in Table IV. According to the conditional probability in Table IV, the maximum value is when $P_m = L$ and SOC = SH, $P_{\text{fc}} = \text{SL}$. Although the probability is not 1, only one case can be selected for the formulation of a rule, which is the pruning of redundant data. Under the previous condition, the frequency of the optimal data "SOC = SH" is the highest. Thus, "SOC = SH" is used as the selected rule. The reason for choosing the data group with the highest probability is that this rule covers more examples, and the output of the learned rule will be closer to a suboptimal result. Therefore, the design of the first rule is completed as follows:

$$\text{if } P_m = L \text{ and SOC} = \text{SH}, \quad \text{then } P_{\text{fc}} = \text{SL}.$$

Before learning the second rule, all examples containing $P_m = L$ and SOC = SH, $P_{\text{fc}} = \text{SL}$ are deleted from the optimal database, and on this basis, the next rule is learned. By analogy, the rules can be traversed and learned according to database sequentially. In addition, it should be noted that implicit rules in the database may not involve all the situations, and the specific rules are designed to solve this problem. For example, when "$P_m = L$, SOC = H" and "$P_m = L$, SOC = SH," the matching output does not exist in the database. When $P_m = \text{SL}$, the range of demand power is negative, and during the solution process of DP, the battery SOC is not maintained at a high state at this time, which is determined by the charging efficiency of the battery and the SOC operating range decided. The fuzzy rule after theoretical optimal learning is shown Table V.

In fact, every rule learned from the global optimal solution can be regarded as an optimal data set. The input attributes of the fuzzy controller have a strong correlation with the output power of the fuel cell. To better describe this relationship, we use a multiple linear regression model to fit the data of each rule [40]

$$Y_i = \theta_0 + \theta_1 x_1 + \theta_2 x_2 + \ldots \theta_m x_m \tag{11}$$

where Y_i is the output power of the fuel cell in rule i, x_m is the mth input value corresponding to the ith rule, and θ_m is the regression coefficient of the ith rule corresponding to input x_m. Since each rule is extracted from multiple data sets, it can be written in matrix form as follows:

$$Y_i = X_i \theta_i \tag{12}$$

$$Y_i = \left[y_1 y_2, \ldots, y_m\right]^T X_i = \begin{bmatrix} 1 & x_{11} & x_{12} & \cdots & x_{1m} \\ 1 & x_{21} & x_{22} & \cdots & x_{2m} \\ \vdots & \vdots & \vdots & \ddots & \vdots \\ 1 & x_{n1} & x_{n2} & \cdots & x_{nm} \end{bmatrix}_{n \times m} \tag{13}$$

where X_i represents the data set included in the ith rule. Each row in X_i represents the specific data in the data set covered by

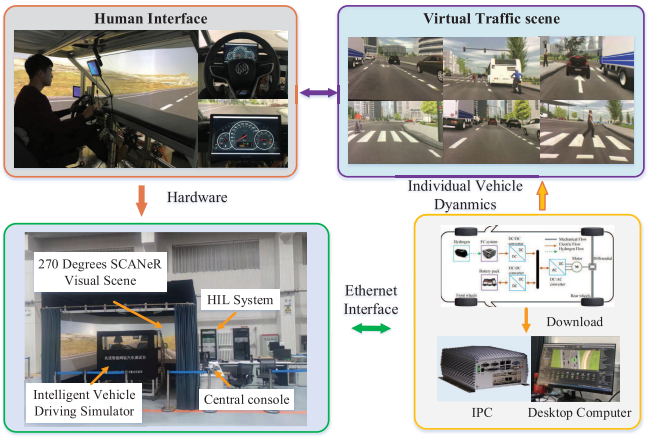

Fig. 7. HIL experiment platform of intelligent connected vehicles.

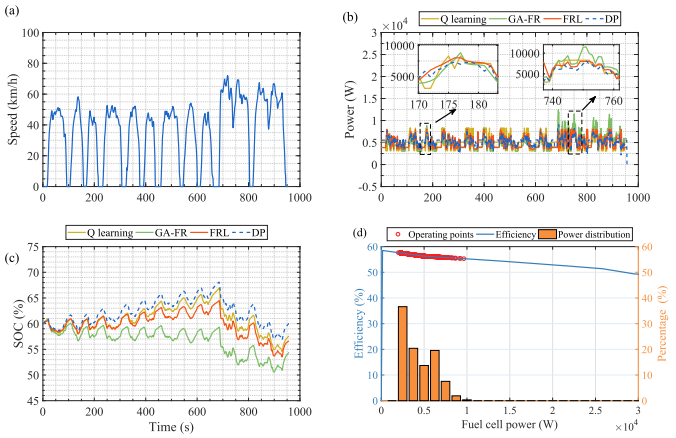

Fig. 8. Q-learning, GA-FR, FRL, and DP power optimization results in Cycle 1. (a) Speed trajectories of Cycle 1. (b) Results of fuel cell power for four strategies. (c) Results of SOC for four strategies. (d) Fuel cell operating points distribution of the FRL algorithm.

the ith rule. m and n indicate that the rule contains input and group data. The normal equation is used to solve the regression coefficient in the above formula

$$\theta_i = \left(X_i{}^T X_i\right)^{-1} X_i{}^T Y_i. \tag{14}$$

After the regression coefficients are solved, we can obtain the output function Y_i of the ith rule. The output result of each function and the membership f_i of each rule are weighted and averaged, and the final solution of the controller can be obtained as follows:

$$\bar{Y} = \frac{Y_1 f_1 + Y_2 f_2 + \cdots + Y_i f_i}{f_1 + f_2 + \cdots + f_i}. \tag{15}$$

At this point, the design of the fuzzy rule controller based on the theoretical optimum is completed.

IV. Evaluation of the Proposed Strategy

In this section, the actual driving trajectories collected under the intelligent connected vehicle test bench and the actual road in Wuhan, China are used to evaluate the energy-saving performance of proposed EMS. Then, the sensitivity and adaptability of the FRL algorithm are summarized and analyzed.

A. Experimental Results in Advanced Intelligent Connected Vehicle Test Bench

The hardware-in-the-loop simulation (HIL) experiment is carried out on the advanced intelligent connected vehicle test bench to restore the largest part of the actual driving situation, which verifies the effectiveness of the proposed EMS. The HIL experiment platform is shown in the Fig. 7. The intelligent connected traffic environment builds virtual traffic conditions based on the software SCANeR to form a complete virtual traffic flow in urban areas. In the virtual traffic environment, the controllable driving of the target vehicle is realized through the human–machine interface, and the power demand of the target vehicle is transmitted to the powertrain system platform to complete the virtual–real combination control and optimization results verification environment. Two drivers with different driving styles drive separately under the same road conditions to obtain two different speed profiles. The speed profiles are named Cycle 1 and 2, respectively.

The genetic algorithm-optimized fuzzy rule (GA-FR) and the Q-learning algorithm are selected for comparison with the proposed strategy of this article, and their design refers to the [48] and [49], respectively. Under the collected actual velocity trajectories Cycle 1, the proposed strategy is compared with GA-FR, Q-learning and DP algorithm to verify the effectiveness, and the results are shown in Fig. 8. These four algorithms have roughly the same fuel cell power trajectories in Cycle 1, and their fuel cell power fluctuates within a small range when the power demand changes. However, when the required power of the vehicle is large, the fuel cell output power of the FRL and DP algorithms is somewhat different. The fuel cell output based on the FRL algorithm is larger than that based on the DP. This is because during rule design, the amount of sample data is small when the required power is large. Most of the required power in the database is below 20 kW, and the proportion of data above 20 kW is small. The fuel cell power of FRL has less fluctuation than that of GA-FR in the high acceleration cases, indicating that the proposed method outperforms GA-FR. The reason is that the FRL performs the repeated incremental pruning based on the decision tree algorithm, which eliminates redundant data and avoid overfitting of rule learning. The other reason is that the input and output of GA-FR are derived from the membership function obtained through iterative learning under driving conditions shown in Fig. 5(a). While in the FRL algorithm, its output is calculated from the optimal data using multiple linear regression model, which can better reflect the characteristics of small fuel cell fluctuations in global energy optimization. Although the genetic algorithm can theoretically achieve the global optimal results, its performance is limited by the selection of initial population and optimization parameters, which may result in a local optimum [50]. In the SOC trajectory of Cycle 1, the change in trend of the SOC of the FRL, Q-learning and DP algorithms is the same, but the SOC obtained by the FRL algorithm varies comparatively more in the vertical direction. The reason for this is that the DP algorithm knows the global driving cycle information. Q-learning-based SOC trajectory is more similar to that of DP than FRL-based,

Fig. 9. Actual urban road line. The line is circular, that is, it starts and ends at the same.

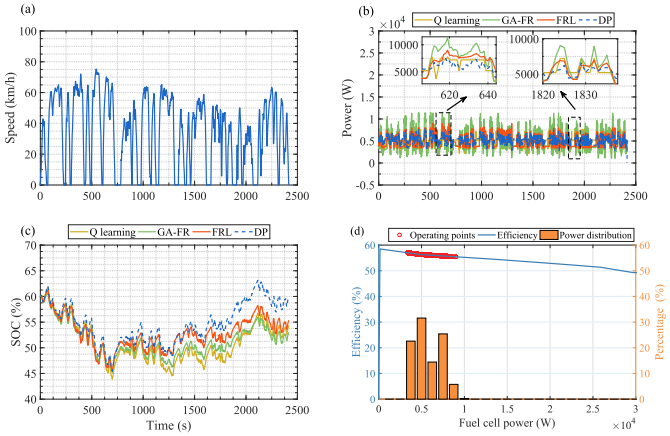

Fig. 10. Q-learning, GA-FR, FRL, and DP power optimization results in WHUC 1. (a) Speed trajectories of WHUC 1. (b) Results of fuel cell power for four strategies. (c) Results of SOC for four strategies. (d) Fuel cell operating points distribution of the FRL algorithm.

because the average power of the fuel cell based on Q-learning is relatively larger in the whole operating condition. To keep the initial and terminal SOC consistent, the battery must follow the law of first charging and then discharging. In addition, the GA-FR-based SOC changes slowly compared with that of the other three algorithms. In Cycle 1, the GA-FR-based SOC decreases by 5.65%, and the FRL and Q-learning based SOC decreases by 3.39% and 2.45%, respectively. Fig. 8(d) depicts the fuel cell operating points in Cycle 1. The fuel cell power distribution in Cycle 1 is more dispersed, and the fuel cell power varies from 3 to 10 kW.

B. Effectiveness and Robustness Analysis of the Proposed Methodology in an Open Traffic Environment

Moreover, the actual velocity trajectories in Wuhan, China are also used to verify the effectiveness of the proposed method. A vehicle is driven on a city route in Wuhan, China, as shown in Fig. 9, which is described by demanded velocity at each point of time. The total length of the route is about 23.2 km, and two speed trajectories of different driving styles are collected, which are named Wuhan Urban Cycle (WHUC) 1 and WHUC 2, respectively. The speed trajectories and optimization results of WHUC 1 are shown in Fig. 10.

In WHUC 1, the similarity of fuel cell power based on FRL, Q-learning and DP is high, and the fuel cell power has a stronger ability to follow the global optimal trajectory. However, based on the GA-FR based strategy, the output power of the fuel cell fluctuates greatly. The reasons for this are the same as mentioned in Section IV-A. From 500 to 750 s and from 1000 to 1250 s of WHUC 1, there are some differences in the fuel cell power of the FRL and DP algorithms. This is because the power demand of the vehicle is relatively high and fluctuates greatly in these stages. The battery power cannot meet the demanded power, and thus, the fuel cell outputs more to meet the driving demand. Q-learning and FRL algorithms have a good performance in inhibiting fuel cell degradation, which is attributed to their good learning ability and adaptability. Before 1500 s of WHUC 1, the SOC trajectories based on FRL and DP basically coincide. In the second half of the driving cycle, it can be observed that the FRL algorithm learns the global optimality of the DP, making the battery constantly charged to maintain the SOC balance. In the first half, the SOC of Q-learning is slightly lower than that of other three algorithms, and then it rises, reaching 54.32% in the final. The frequency and efficiency of the fuel cell operating points in the WHUC 1 according to the FRL strategy are shown in Fig. 10(d). The fuel cell power varies from 3 to 10 kW, and the operating point is mainly concentrated at approximately 5 kW, thus maintaining a high efficiency. Through the above verification and analysis, the FRL algorithm has learned the global optimality from DP, and can guarantee optimal control. Moreover, the results in the advanced intelligent connected vehicle test bench and open traffic environment show that the proposed methodology has good robustness and maintains the battery SOC in a better range.

C. Comparison of Equivalent Hydrogen Consumption

Evaluating the quality of an EMS ultimately comes down to hydrogen consumption. The rule-based strategy referred to the [38] is selected for comparison with the proposed strategy. For a fair comparison, the equivalent hydrogen consumption m_{b,H_2} of the battery is introduced to consider the final SOC change as follows [51]:

$$m_{b,H_2} = \frac{\Delta \mathrm{SOC} \cdot E_b \cdot 3600}{\eta_{\mathrm{fc}} \cdot Q_m}. \tag{16}$$

Table VI shows the hydrogen consumption of four strategies in different driving cycles. The hydrogen consumption calculated by FRL have a difference of less than 1.12%–4.13% with DP, while the hydrogen improvement is in the range of 8.48%–10.71% compared with the rule-based strategy. The energy saving effect of FRL is about 1% higher than that of GA-FR, and it is also slightly better than the Q-learning algorithm. Therefore, the superior performance of the proposed strategy reaching a remarkable reduction in hydrogen consumption, especially in urban driving cycles.

D. Sensitivity Analysis of the FRL Algorithm

The component size can determine the energy-saving effect of an EMS [23], [52], [53]. Sections IV-A and IV-B studies the energy-saving effect when the battery capacity is fixed, but changing the battery capacity will affect the distribution

TABLE VI

HYDROGEN CONSUMPTION RESULTS OBTAINED WITH THE SET OF TESTED STRATEGIES IN DIFFERENT DRIVING CYCLES

Cycle name	Method	Final SOC (%)	Consumption (g)
Cycle 1	DP	60	76.13
	FRL	56.61	77.03 (+1.18%)
	Q-learning	57.55	77.49 (+1.79 %)
	GA-FR	54.35	78.37 (+2.94 %)
	Rule-based	55.07	84.16 (+10.55%)
Cycle 2	DP	60	96.03
	FRL	52.16	99.27 (+3.37%)
	Q-learning	50.94	99.15 (+3.25 %)
	GA-FR	48.97	99.81(+3.94 %)
	Rule-based	46.54	110.28 (+14.84%)
WHUC 1	DP	60	190.78
	FRL	55.33	192.76 (+1.04%)
	Q-learning	54.32	193.09 (+1.21 %)
	GA-FR	52.94	195.53 (+2.49 %)
	Rule-based	51.03	210.27 (+10.21 %)
WHUC 2	DP	60	196.33
	FRL	56.74	198.83 (+1.28%)
	Q-learning	54.67	199.69(+1.71 %)
	GA-FR	52.71	201.13(+2.45 %)
	Rule-based	51.78	215.64 (+9.84 %)

of energy. This section discusses the difference for different battery capacities between the FRL-based EMS and optimal hydrogen consumption, and analyses the sensitivity of FRL to battery capacity.

The battery capacity is changed by changing the number of connections in parallel. The optional parameters of the battery are 2.102, 4.205, and 6.31 kWh, whose corresponding capacities are 6, 12, and 18 Ah, respectively. The energy saving effect of FRL is analyzed in Cycle 1 and 2, and the results are shown in Table VII. In Cycle 1 and 2, the hydrogen consumption of the FRL-based EMS decreases as the battery capacity increases, and the difference from the optimal value decreases. Fig. 11 shows the database clustering results that the battery energy is 4.205 and 6.31 kWh, respectively. Compared with Fig. 6(a), the clustering results of power demand in Fig. 11 show little change, because the increase in battery energy leads to a small increase in vehicle mass and a slight increase in power demand. However, the clustering results of SOC and fuel cell power vary greatly. As the battery energy increases, the battery output power increases, resulting in a low output power of the fuel cell. The clustering results show that battery energy is 2.102 kWh are dispersed, while the clustering results of fuel cell power for 4.205 and 6.31 kWh of battery energy are increasingly concentrated, leading to the shift of the operating point of the fuel cell to the high-efficiency zone. Thus, the overall energy saving effect improves.

E. Adaptability Analysis of the FRL Algorithm

As mentioned in Section IV-D, when the powertrain system parameters change, the corresponding energy distribution law also changes. After changing the battery capacity, it is necessary to reestablish the optimal database, reclassify the data,

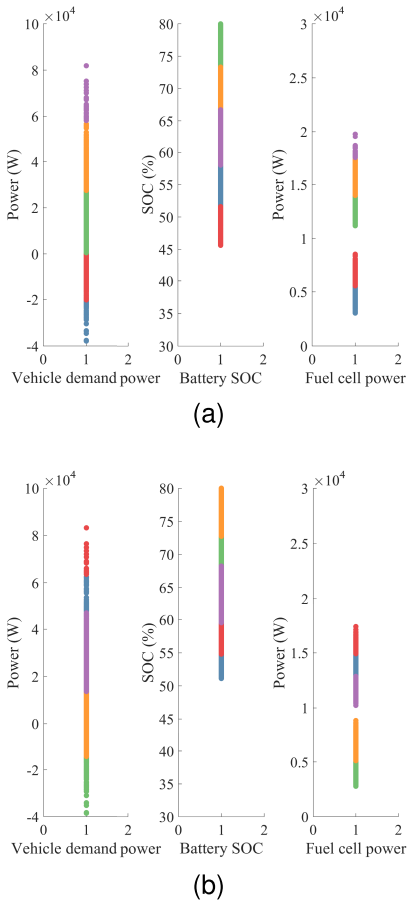

Fig. 11. Database clustering results. (a) Battery energy is 4.205 kWh. (b) Battery energy is 6.31 kWh.

TABLE VII

COMPARISON OF HYDROGEN CONSUMPTION RESULTS FOR DIFFERENT BATTERY CAPACITIES

Cycle	Capacity (kWh)	Method	Consumption (g)
Cycle 1	6	DP	76.13
	6	FRL	77.03 (+1.18%)
Cycle 1	12	DP	76.03
	12	FRL	76.81 (+1.026%)
Cycle 1	18	DP	76.44
	18	FRL	77.23 (+1.034%)
Cycle 2	6	DP	96.03
	6	FRL	99.27 (+3.37%)
Cycle 2	12	DP	92.78
	12	FRL	94.65 (+2.00%)
Cycle 2	18	DP	92.42
	18	FRL	94.00 (+1.71%)

and reextract and learn the rules. This section simplifies the above process and applies the fuzzy rule learned for a battery capacity of 6 Ah to powertrain systems with different battery capacities. Meanwhile, as a comparison, the results applied to the corresponding battery capacity when the corresponding database is changed are also given.

The adaptability of the proposed strategy to different battery parameters is verified under Cycle 1 and 2, which is demonstrated by comparing the hydrogen consumption optimized by DP. The difference in hydrogen consumption $\eta_{h,\mathrm{dif}}$ is defined

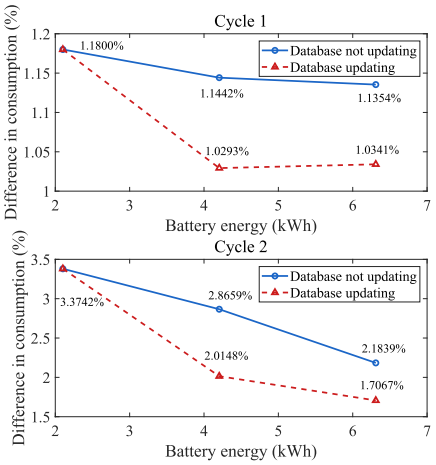

Fig. 12. Difference in hydrogen consumption between FRL and DP.

as [23] follows:

$$\eta_{h,\mathrm{dif}} = \frac{J_{\mathrm{FRL}} - J_{\mathrm{DP}}}{J_{\mathrm{DP}}} \tag{17}$$

where J_{FRL} denotes the total equivalent hydrogen consumption of FRL and J_{DP} is the total hydrogen consumption of DP. The results are shown in Fig. 12. The blue solid line shows the results when the fuzzy rules learned for a battery capacity of 6 Ah are applied to 6, 12, and 18 Ah. The brown dotted line shows the results when the fuzzy rules learned for a battery capacity of 6, 12, and 18 Ah are applied corresponding to 6, 12, and 18 Ah, respectively. It can be seen from the blue solid line that in the two driving cycles, as the battery capacity increases, the energy-saving effect of the proposed strategy improves. In Cycle 1, the energy-saving effect decreases from 1.18% to 1.13%, while in Cycle 2, the energy-saving effect decreases from 3.37% to 2.18%. Moreover, when the battery capacity is 18 Ah, the fuzzy rules are learned under this parameter and then applied under this parameter. The energy-saving effect eventually drops to 1.03% and 1.71% in Cycle 1 and 2, respectively, which shows that learning under the same battery capacity, and then verifying under this parameter, the energy-saving effect is better. However, it has little effect on energy savings whether or not the rules are updated when the battery capacity changes. In Cycle 1 and 2, this difference is about only 0.1% and 0.8%, respectively.

Through the above analysis, the conclusion can be drawn that the FRL-based EMS still maintains a good energy-saving effect for the powertrain system under different battery capacities. The energy-saving effect of an algorithm is greatly affected by changes (such as component aging) in the system model in practical applications. The main goal of this article is to solve the real-time energy optimization problem for FCEVs. The methodology presented in this article can be used to address algorithmic performance degradation due to system model changes. The output characteristics of the energy source can be used to identify whether components are aging, resulting in changes in model parameters. Specifically, a degradation model of an FCS can be built based on the decrease of voltage. Moreover, the polarization curve can be determined by the decrease in voltage at a rated current, and it is easy to measure the voltage of a fuel cell. Then the degree of fuel cells degradation can be calculated from voltage degradation at the rated current to determine the state of health. The fuzzy rule controller can add an input dimension to identify whether the fuel cell internal voltage degrade. Finally, the efficiency curves and hydrogen consumption of fuel cells can be obtained based on the state of health. The voltage of the FCS can therefore be measured to identify the degree of degradation of the fuel cell, and then the different energy management strategies can be designed based on the degree of degradation to adapt to changes in the internal parameters of the fuel cell. For more information about the degradation-adaptive EMSs, please refer to [54]. Similarly, this idea is also suitable for batteries. Moreover, the energy management problem of electric vehicles is a common requirement of hybrid powertrain system, this strategy can be applied to hybrid electric vehicles with other powertrain architectures. It is also promising to apply this methodology to the field of power generation.

V. Conclusion

A FRL-based EMS is investigated to improve the hydrogen economy and SOC maintenance capability of FCEVs. Firstly, the DP algorithm is applied to solve the offline energy optimization and establishing the optimal database. Then, the fuzzy rules are extracted from the optimal database and the membership function is designed by hierarchical clustering. The multiple linear regression model is applied to fit the parameters of each rule. The results promise a reduction in hydrogen consumption by approximately 1.5% and 10% compared with the rule-based strategy and the GA-FR, and they are close to or slightly better than Q-learning algorithm. We also demonstrate that the energy-saving effect approaches the theoretical optimum as battery capacity increases. Moreover, the algorithm can still achieve good hydrogen economy when the parameters of the vehicle power system are changed, such as the battery capacity.

We also acknowledge the limitations that the performance of the proposed method depends on the accuracy of the system model, because the fuzzy rules are learned through the optimal database obtained by the DP algorithm. When the model accuracy is poor, the energy-saving performance of the fuzzy controller may be reduced. In addition, the proposed method cannot handle the model imprecision and uncertainty. To ensure the effectiveness of the method, the simulation model accuracy for the optimal database based on DP must be guaranteed to a certain extent. Moreover, the offline simulation results can be compared with the actual experimental results to obtain more accurate data, so that the database can be matched as closely as possible with the actual dynamics of the system, and then do rule learning on this basis.

References

[1] H. Peng, J. Li, L. Löwenstein, and K. Hameyer, "A scalable, causal, adaptive energy management strategy based on optimal control theory for a fuel cell hybrid railway vehicle," *Appl. Energy*, vol. 267, Jun. 2020, Art. no. 114987.

[2] J. Zhou, J. Liu, Y. Xue, and Y. Liao, "Total travel costs minimization strategy of a dual-stack fuel cell logistics truck enhanced with artificial potential field and deep reinforcement learning," *Energy*, vol. 239, Jan. 2022, Art. no. 121866.

[3] X. Wu, X. Hu, X. Yin, L. Li, Z. Zeng, and V. Pickert, "Convex programming energy management and components sizing of a plug-in fuel cell urban logistics vehicle," *J. Power Sources*, vol. 423, pp. 358–366, May 2019.

[4] Q. Xun, N. Murgovski, and Y. Liu, "Chance-constrained robust co-design optimization for fuel cell hybrid electric trucks," *Appl. Energy*, vol. 320, Aug. 2022, Art. no. 119252.

[5] Q. Xun, N. Murgovski, and Y. Liu, "Joint component sizing and energy management for fuel cell hybrid electric trucks," *IEEE Trans. Veh. Technol.*, vol. 71, no. 5, pp. 4863–4878, May 2022.

[6] R. Rodriguez, J. P. F. Trovão, and J. Solano, "Fuzzy logic-model predictive control energy management strategy for a dual-mode locomotive," *Energy Convers. Manage.*, vol. 253, Feb. 2022, Art. no. 115111.

[7] J. Gao, M. Li, Y. Hu, H. Chen, and Y. Ma, "Challenges and developments of automotive fuel cell hybrid power system and control," *Sci. China Inf. Sci.*, vol. 62, no. 5, pp. 1–25, May 2019.

[8] X. Hu, C. Zou, X. Tang, T. Liu, and L. Hu, "Cost-optimal energy management of hybrid electric vehicles using fuel cell/battery health-aware predictive control," *IEEE Trans. Power Electron.*, vol. 35, no. 1, pp. 382–392, Jan. 2020.

[9] R. Koubaa and L. Krichen, "Double layer metaheuristic based energy management strategy for a fuel cell/ultra-capacitor hybrid electric vehicle," *Energy*, vol. 133, pp. 1079–1093, Aug. 2017.

[10] B. M. Duan, Q. N. Wang, J. N. Wang, X. N. Li, and T. Ba, "Calibration efficiency improvement of rule-based energy management system for a plug-in hybrid electric vehicle," *Int. J. Automot. Technol.*, vol. 18, no. 2, pp. 335–344, Apr. 2017.

[11] B.-H. Nguyen, T. Vo-Duy, M. C. Ta, and J. P. F. Trovao, "Optimal energy management of hybrid storage systems using an alternative approach of Pontryagin's minimum principle," *IEEE Trans. Transport. Electrific.*, vol. 7, no. 4, pp. 2224–2237, Dec. 2021.

[12] Q. Xun, V. Roda, Y. Liu, X. Huang, and R. Costa-Castelló, "An adaptive power split strategy with a load disturbance compensator for fuel cell/supercapacitor powertrains," *J. Energy Storage*, vol. 44, Dec. 2021, Art. no. 103341.

[13] X. Tang, J. Chen, T. Liu, Y. Qin, and D. Cao, "Distributed deep reinforcement learning-based energy and emission management strategy for hybrid electric vehicles," *IEEE Trans. Veh. Technol.*, vol. 70, no. 10, pp. 9922–9934, Oct. 2021.

[14] G. Du, Y. Zou, X. Zhang, T. Liu, J. Wu, and D. He, "Deep reinforcement learning based energy management for a hybrid electric vehicle," *Energy*, vol. 201, Jun. 2020, Art. no. 117591.

[15] T. Hofman, R. M. van Druten, A. F. A. Serrarens, and M. Steinbuch, "Rule-based energy management strategies for hybrid vehicles," *Int. J. Electr. Hybrid Veh.*, vol. 1, no. 1, pp. 71–94, 2007.

[16] L. Xu, J. Li, M. Ouyang, J. Hua, and G. Yang, "Multi-mode control strategy for fuel cell electric vehicles regarding fuel economy and durability," *Int. J. Hydrogen Energy*, vol. 39, no. 5, pp. 2374–2389, Feb. 2014.

[17] M. Sorrentino, C. Pianese, and M. Cilento, "A specification independent control strategy for simultaneous optimization of fuel cell hybrid vehicles design and energy management," *IFAC-PapersOnLine*, vol. 49, no. 11, pp. 369–376, 2016.

[18] F. Odeim, J. Roes, L. Wülbeck, and A. Heinzel, "Power management optimization of fuel cell/battery hybrid vehicles with experimental validation," *J. Power Sources*, vol. 252, pp. 333–343, Apr. 2014.

[19] H. Yin, W. Zhou, M. Li, C. Ma, and C. Zhao, "An adaptive fuzzy logic-based energy management strategy on battery/ultracapacitor hybrid electric vehicles," *IEEE Trans. Transport. Electrific.*, vol. 2, no. 3, pp. 300–311, Sep. 2016.

[20] H. Zhang, J. Peng, H. Tan, H. Dong, and F. Ding, "A deep reinforcement learning-based energy management framework with Lagrangian relaxation for plug-in hybrid electric vehicle," *IEEE Trans. Transport. Electrific.*, vol. 7, no. 3, pp. 1146–1160, Sep. 2021.

[21] L. Guo, H. Chen, B. Gao, and Q. Liu, "Energy management of HEVs based on velocity profile optimization," *Sci. China Inf. Sci.*, vol. 62, no. 8, pp. 1–3, Aug. 2019.

[22] H. F. Gharibeh, A. S. Yazdankhah, and M. R. Azizian, "Energy management of fuel cell electric vehicles based on working condition identification of energy storage systems, vehicle driving performance, and dynamic power factor," *J. Energy Storage*, vol. 31, Oct. 2020, Art. no. 101760.

[23] S. Hou, J. Gao, Y. Zhang, M. Chen, J. Shi, and H. Chen, "A comparison study of battery size optimization and an energy management strategy for FCHEVs based on dynamic programming and convex programming," *Int. J. Hydrogen Energy*, vol. 45, no. 41, pp. 21858–21872, Aug. 2020.

[24] K. Song, X. Wang, F. Li, M. Sorrentino, and B. Zheng, "Pontryagin's minimum principle-based real-time energy management strategy for fuel cell hybrid electric vehicle considering both fuel economy and power source durability," *Energy*, vol. 205, Aug. 2020, Art. no. 118064.

[25] Z. Chen, C. C. Mi, R. Xiong, J. Xu, and C. You, "Energy management of a power-split plug-in hybrid electric vehicle based on genetic algorithm and quadratic programming," *J. Power Sources*, vol. 248, no. 15, pp. 416–426, Feb. 2014.

[26] Y. Wu, J. Zhang, and T. Shen, "A logical network approximation to optimal control on a continuous domain and its application to HEV control," *Sci. China Inf. Sci.*, vol. 65, no. 11, pp. 1–18, Nov. 2022.

[27] B. Geng, J. K. Mills, and D. Sun, "Two-stage energy management control of fuel cell plug-in hybrid electric vehicles considering fuel cell longevity," *IEEE Trans. Veh. Technol.*, vol. 61, no. 2, pp. 498–508, Feb. 2012.

[28] D. F. Pereira, F. D. C. Lopes, and E. H. Watanabe, "Nonlinear model predictive control for the energy management of fuel cell hybrid electric vehicles in real time," *IEEE Trans. Ind. Electron.*, vol. 68, no. 4, pp. 3213–3223, Apr. 2021.

[29] Q. Zhou, D. Zhao, B. Shuai, Y. Li, H. Williams, and H. Xu, "Knowledge implementation and transfer with an adaptive learning network for real-time power management of the plug-in hybrid vehicle," *IEEE Trans. Neural Netw. Learn. Syst.*, vol. 32, no. 12, pp. 5298–5308, Dec. 2021.

[30] Q. Zhou et al., "Multi-step reinforcement learning for model-free predictive energy management of an electrified off-highway vehicle," *Appl. Energy*, vol. 255, Dec. 2019, Art. no. 113755.

[31] B. Xu et al., "Parametric study on reinforcement learning optimized energy management strategy for a hybrid electric vehicle," *Appl. Energy*, vol. 259, Feb. 2020, Art. no. 114200.

[32] J. Wu, H. He, J. Peng, Y. Li, and Z. Li, "Continuous reinforcement learning of energy management with deep Q network for a power split hybrid electric bus," *Appl. Energy*, vol. 222, pp. 799–811, Jul. 2018.

[33] R. Lian, J. Peng, Y. Wu, H. Tan, and H. Zhang, "Rule-interposing deep reinforcement learning based energy management strategy for power-split hybrid electric vehicle," *Energy*, vol. 197, Apr. 2020, Art. no. 117297.

[34] H. Sun, Z. Fu, F. Tao, L. Zhu, and P. Si, "Data-driven reinforcement-learning-based hierarchical energy management strategy for fuel cell/battery/ultracapacitor hybrid electric vehicles," *J. Power Sources*, vol. 455, Apr. 2020, Art. no. 227964.

[35] C. Qi et al., "Hierarchical reinforcement learning based energy management strategy for hybrid electric vehicle," *Energy*, vol. 238, Jan. 2022, Art. no. 121703.

[36] X. Hu, J. Han, X. Tang, and X. Lin, "Powertrain design and control in electrified vehicles: A critical review," *IEEE Trans. Transport. Electrific.*, vol. 7, no. 3, pp. 1990–2009, Feb. 2021.

[37] S. Hou, H. Chen, Y. Zhang, and J. Gao, "Speed planning and energy management strategy of hybrid electric vehicles in a car-following scenario," *Control Theory Technol.*, vol. 20, no. 2, pp. 185–196, May 2022.

[38] H. He, X. Wang, J. Chen, and Y.-X. Wang, "Regenerative fuel cell-battery-supercapacitor hybrid power system modeling and improved rule-based energy management for vehicle application," *J. Energy Eng.*, vol. 146, no. 6, Dec. 2020, Art. no. 4020060.

[39] Y. Liu, J. Liu, Y. Zhang, Y. Wu, Z. Chen, and M. Ye, "Rule learning based energy management strategy of fuel cell hybrid vehicles considering multi-objective optimization," *Energy*, vol. 207, Sep. 2020, Art. no. 118212.

[40] Y. Liu, J. Liu, D. Qin, G. Li, Z. Chen, and Y. Zhang, "Online energy management strategy of fuel cell hybrid electric vehicles based on rule learning," *J. Cleaner Prod.*, vol. 260, Jul. 2020, Art. no. 121017.

[41] H. Jia, J. Tang, Y. Yu, Y. Sun, B. Yin, and C. Zhang, "Energy management strategy of fuel cell/battery hybrid vehicle based on series fuzzy control," *Int. J. Automot. Technol.*, vol. 22, no. 6, pp. 1545–1556, Dec. 2021.

[42] X. Han, F. Li, T. Zhang, T. Zhang, and K. Song, "Economic energy management strategy design and simulation for a dual-stack fuel cell electric vehicle," *Int. J. Hydrogen Energy*, vol. 42, no. 16, pp. 11584–11595, Apr. 2017.

[43] K. Simmons, Y. Guezennec, and S. Onori, "Modeling and energy management control design for a fuel cell hybrid passenger bus," *J. Power Sources*, vol. 246, pp. 736–746, Jan. 2014.

[44] X. Zhao and G. Guo, "Braking torque distribution for hybrid electric vehicles based on nonlinear disturbance observer," *Proc. Inst. Mech. Eng., D, J. Automobile Eng.*, vol. 233, no. 13, pp. 3327–3341, Nov. 2019.
[45] Y. Liu, J. Li, Z. Chen, D. Qin, and Y. Zhang, "Research on a multi-objective hierarchical prediction energy management strategy for range extended fuel cell vehicles," *J. Power Sources*, vol. 429, pp. 55–66, Jul. 2019.
[46] A. H. Ganesh and B. Xu, "A review of reinforcement learning based energy management systems for electrified powertrains: Progress, challenge, and potential solution," *Renew. Sustain. Energy Rev.*, vol. 154, Feb. 2022, Art. no. 111833.
[47] A. Biswas, P. G. Anselma, and A. Emadi, "Real-time optimal energy management of multimode hybrid electric powertrain with online trainable asynchronous advantage actor–critic algorithm," *IEEE Trans. Transport. Electrific.*, vol. 8, no. 2, pp. 2676–2694, Jun. 2022.
[48] C. Wang, R. Liu, and A. Tang, "Energy management strategy of hybrid energy storage system for electric vehicles based on genetic algorithm optimization and temperature effect," *J. Energy Storage*, vol. 51, Jul. 2022, Art. no. 104314.
[49] T. Liu, Y. Zou, D. Liu, and F. Sun, "Reinforcement learning of adaptive energy management with transition probability for a hybrid electric tracked vehicle," *IEEE Trans. Ind. Electron.*, vol. 62, no. 11, pp. 7837–7846, Dec. 2015.
[50] X. Hu, J. Han, X. Tang, and X. Lin, "Powertrain design and control in electrified vehicles: A critical review," *IEEE Trans. Transport. Electrific.*, vol. 7, no. 3, pp. 1990–2009, Feb. 2021.
[51] D. Zhou, A. Al-Durra, F. Gao, A. Ravey, I. Matraji, and M. G. Simões, "Online energy management strategy of fuel cell hybrid electric vehicles based on data fusion approach," *J. Power Sources*, vol. 366, pp. 278–291, Oct. 2017.
[52] Y. Li, X. Tang, X. Lin, L. Grzesiak, and X. Hu, "The role and application of convex modeling and optimization in electrified vehicles," *Renew. Sustain. Energy Rev.*, vol. 153, Jan. 2022, Art. no. 111796.
[53] L. Zhang, X. Hu, Z. Wang, F. Sun, J. Deng, and D. G. Dorrell, "Multiobjective optimal sizing of hybrid energy storage system for electric vehicles," *IEEE Trans. Veh. Technol.*, vol. 67, no. 2, pp. 1027–1035, Feb. 2018.
[54] K. Song, Y. Ding, X. Hu, H. Xu, Y. Wang, and J. Cao, "Degradation adaptive energy management strategy using fuel cell state-of-health for fuel economy improvement of hybrid electric vehicle," *Appl. Energy*, vol. 285, Mar. 2021, Art. no. 116413.

Shengyan Hou received the M.Eng. degree in control engineering from the Jilin University, Changchun, China, in 2020, where he is currently pursuing the Ph.D. degree in control science and engineering.

His current research focuses on optimal control of intelligent-connected vehicles.

Hai Yin received the B.S. degree in automation and the M.Eng. and Ph.D. degrees in control science and engineering from the Harbin Institute of Technology, Harbin, China, in 2005, 2007, and 2015, respectively.

From 2007 to 2016, she was an Engineer with the Institute of Basic and Cross-Cutting Sciences. She is currently a Senior Engineer with the State Key Laboratory of Automotive Simulation and Control, Jilin University, Changchun, China. Her research interests include automotive control and nonlinear control.

Benjamín Pla received the B.Eng. degree in industrial engineering from the Universitat Politécnica de Valéncia (UPV), Valencia, Spain, in 2004, and the Ph.D. degree from the Research Institute CMT-Motores Térmicos, Valencia, in 2009.

During this process, he passed through different research grants until receiving a Lecturer position in 2008. He is currently an Associate Professor, giving lectures on thermodynamics and fluid-mechanics in the Aerospace Degree of the UPV. His research activities are a part of the Engine Control Research Group with CMT-Motores Térmicos. His research interest is focused on the control and diagnosis of vehicle powertrains.

Jinwu Gao received the B.Eng. degree from the Department of Automation Measurement and Control Engineering, Harbin Institute of Technology, Harbin, China, in 2005, and the Ph.D. degree from the Department of Control Science and Engineering, Harbin Institute of Technology, in 2012.

From 2012 to 2014, he was an Assistant Professor with Sun Yat-sen University, Guangzhou, China. In July 2014, he held a post-doctoral position with the Department of Engineering and Applied Science, Sophia University, Tokyo, Japan. From 2016 to 2020, he was an Associate Professor with Jilin University, Changchun, China, where he has been a Professor since September 2020. His research interests include control theory and application in automotive powertrain.

Hong Chen (Fellow, IEEE) received the B.S. and M.S. degrees in process control from Zhejiang University, Hangzhou, China, in 1983 and 1986, respectively, and the Ph.D. degree in system dynamics and control engineering from the University of Stuttgart, Stuttgart, Germany, in 1997.

In 1986, she joined the Jilin University, Changchun, China. From 1993 to 1997, she was a Wissenschaftlicher Mitarbeiter with the Institut für Systemdynamik und Regelungstechnik, University of Stuttgart. Since 1999, she has been a Professor at Jilin University and hereafter a Tang Aoqing Professor. From 2015 to 2019, she served as the Director of the State Key Laboratory of Automotive Simulation and Control. In 2019, she joined Tongji University as a Distinguished Professor. Her current research interests include model predictive control, nonlinear control, and applications in mechatronic systems focusing on automotive systems.